International Journal of Stem Cells Vol. 7, No. 2, 2014 http://dx.doi.org/10.15283/ijsc.2014.7.2.79

ORIGINAL ARTICLE

Possible Local Stem Cells Activation by Microcurrent Application in Experimentally Injured Soleus Muscle

Maha Baligh Zickri

Department of Histology, Faculty of Medicine, Cairo University, Cairo, Egypt

Background: Severe injuries in skeletal muscle result in muscle weakness that delays recovery and contribute to progressive decline in muscle function. Microcurrent therapy (MCT) is a novel treatment method used in soft tissue injury and tissue regeneration therapy. The regenerative capacity of skeletal muscle tissue resides in satellite cells, the quiescent adult stem cells.

Aim: The present work aimed at investigating the relation between microcurrent therapy and local stem cells in regeneration of induced skeletal muscle injury in albino rat.

Materials and methods: Twenty six adult male albino rats were divided into Sham group, Injury group (I): subjected to soleus muscle injury and subdivided into subgroups I1 & I2 sacrificed 2 and 4 weeks after injury respectively. Microcurrent group (M): subjected to muscle injury and micro-current was applied. The animals were subdivided into subgroups M1 and M2 sacrificed 2 and 4 weeks after injury. Histological, immunohistochemical and morphometric studies were performed.

Results: Atypical fibers widely separated by infiltrating cells and strong acidophilic sarcoplasm with focal vacuolations were found in injury group. In M1 subgroup few atypical fibers were found. In M2 subgroup multiple typical fibers were detected. A significant decrease in the mean area of atypical fibers, a significant increase in the mean area% of alpha SMA+ve cells and that of CD34+ve cells were found in microcurrent group compared to injury group.

Conclusion: A definite therapeutic effect of the microcurrent was found on induced skeletal muscle injury. This effect was proved to be related to satellite cell activation.

Keywords: Skeletal muscle, Injury, Microcurrent, Satellite cells

Introduction

Severe injuries in skeletal muscle result in muscle weakness that delays recovery, which exposes patients to neuromuscular complications that increase hospital stay and mortality (1). In muscular dystrophy, an imbalance between muscle damage and muscle repair through stem-cell mediated regeneration is thought to contribute to progressive decline in muscle function (2).

Microcurrent therapy (MCT) is a novel treatment for soft tissue injury, where the MCT showed better therapeutic compliance than traditional therapy (3). Regeneration therapy device which produces a microcurrent range was used for treatment of chronic wounds and ulcers associated with chronic diseases as diabetes mellitus (4). Recently, high therapeutic efficiency of cell-stimulation with low-intensity electric current was proved in inflammatory conditions (5).

Satellite cells (Scs) have been distinguished by immunostaining and expression of CD34 surface receptors including (6). These cells are activated in response to in-

Accepted for publication July 25, 2014, Published online November 30, 2014
Correspondence to **Maha Baligh Zickri**
Department of Histology, Faculty of Medicine, Cairo University, Cairo, Egypt
Tel: +20123955078, Fax: +82-20235381183, +20235381760
E-mail: maha_kaah@yahoo.com

jury and undergo cell division (7). Recently, it was confirmed that the regenerative capacity of skeletal muscle tissue resides in satellite cells, the quiescent adult stem cells (8).

The present work aimed at investigating the relation between microcurrent therapy and local stem cells in regeneration of induced skeletal muscle injury in albino rat.

Materials and Methods

The study was conducted at the **Animal House of Kasr El Aini, Faculty of Medicine, Cairo University, according to the guide for the care and use of laboratory animals.**

Experimental design

Twenty six male albino rats weighing 150～200 g were housed in a temperature and light-controlled room, with free access to food and water. The animals were classified into the following groups, which were kept in separate cages:

Sham group (S Group): Included 6 rats receiving anaesthesia but not undergoing injury of gastrocnemius-soleus muscle. **S1 subgroup** 3 rats sacrificed 2 weeks later. **S2 subgroup** 3 rats sacrificed 4 weeks later.

Injury group (I Group): Included 10 rats subjected to soleus muscle injury without any treatment procedures, other than the routine care of the wound. Betadine was applied to the wound site and rinsing with normal saline was performed at the site of injury on daily base. To induce anesthesia, ketamine hydrochloride (Ketalar, (Parke Davis Barcelona, Spain) (35 mg/kg) was injected into the gluteus maximus muscle of the animal. Using aseptic techniques, a 3 cm longitudinal skin incision was made along the leg. Then an incision (1 cm in length) was made perpendicular to the orientation of the muscle. The fascia and skin were sutured (9). Daily aseptic dressing was applied on the wound. The animals were subdivided into 2 subgroups:

Subgroup I1: 5 rats sacrificed 2 weeks following the day of injury.

Subgroup I2: 5 rats sacrificed four weeks following the day of injury.

Microcurrent group (M Group): Included 10 rats subjected to soleus muscle injury by the same protocol as in I group. Micro-current electric stimulator, model EMSI-4250 (made in Taiwan) was used for the treatment. Intensity was 100 microampere (10) and the frequency 10 Hz. Clip electrodes were used and microcurrent therapy was applied 3 sessions/week (11). The negative lead (1.0×1.0 cm) was placed over the muscle injury site, while the positive lead was placed proximally on the thigh region of the same side. The microcurrent was applied for 20 minutes in each session (12). The animals were subdivided into 2 subgroups:

Subgroup M1: 5 rats sacrificed 2 weeks following the day of injury.

Subgroup M2: 5 rats sacrificed four weeks following the day of injury.

The animals were sacrificed by a lethal dose of ether. Soleus muscle was exposed and muscle specimens were placed in 10% formol saline. 5 microns thick sections were prepared and subjected to the following studies.

Hematoxylin and eosin (13)

Immunohistochemical (IHC) Study

Anti-alpha smooth muscle actin (α-SMA) immunostaining: The marker for this antibody stains smooth muscle cells in vessel walls, gut wall, myometrium and myoepithelial cells. Anti-alpha smooth muscle actin antibody (Rabbit polyclonal antibody) (ab5694) was used at a concentration 0.5～2 μg/ml. Perform heat mediated antigen retrieval before commencing with IHC staining protocol. Glioma tissue sections were used as positive control specimens. Cellular localization is the cytoplasm. On the other hand, one of the muscle sections was used as a negative control by passing the step of applying the primary antibody (14).

CD34 immunostaining is the marker for hematopoietic progenitor cells, small vessel endothelium (15) and satellite cells of skeletal muscle (16) of a variety of tissues. CD34 goat polyclonal Ab (Sigma-Aldrich Chemie Corporation laboratories, Germany, catalogue ID SAB4300690). The sections were treated with CD34, at 5～15 μg/ml ready to use at room temperature. Cellular localization is the cell membrane. Tonsil sections were used as positive control specimens. On the other hand, one of the muscle sections was used as a negative control by passing the step of applying the primary antibody.

Morphometric study

Using Leica Qwin 500 LTD computer assisted image analysis system (Cambridge, United Kingdom), the area of atypical muscle fibers was estimated in 10 low power fields (LPF) in control and experimental groups using interactive measurements menu. The area% of α SMA positive (+ve) cells and CD34 +ve cells were measured in 10 high power fields using binary mode.

Statistical analysis

Quantitative data were summarized as means and standard deviations and compared using one-way analysis-of-

variance (ANOVA). Any significant ANOVA was followed by Bonferroni post-hoc test to detect which pairs of groups caused the significant difference. p-values <0.05 were considered statistically significant. Calculations were made on SPSS 9,0 software (17).

Results

Histological results

Skeletal muscle sections of **S group** showed longitudinal muscle fibers (Fig. 1A) that exhibited oval pale nuclei and transverse striations in the sarcoplasm (Fig. 1B). In **subgroup I1** (Sacrifice 2weeks following muscle injury) the injured area demonstrated atypical fibers widely separated by infiltrating cells. Most fibers contained dark nuclei. Distended capillaries were noted (Fig. 2A). The fibers revealed partial loss of striations and some fibers recruited strong acidophilic sarcoplasm with focal vacuolations on close observation (Fig. 2B). In **subgroup I2** (Sacrifice 4 weeks following muscle injury), atypical fibers appeared separated by few infiltrating cells. Some fibers exhibited dark nuclei (Fig. 3A). Partial loss of striations was found

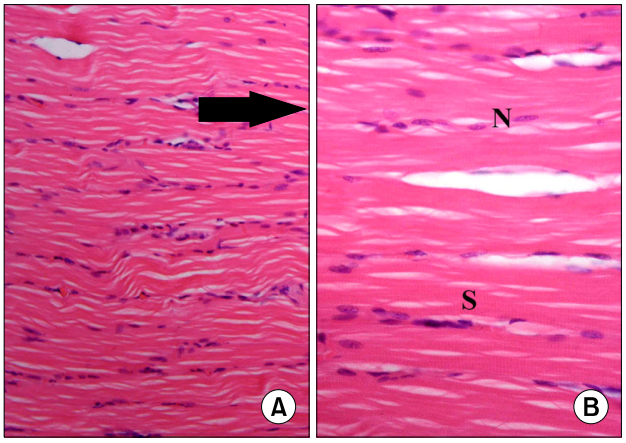

Fig. 1. (A) Skeletal muscle section of S group showing longitudinal muscle fibers (arrows) (H&E, ×200). (B) Higher magnification of the previous figure showing oval pale nuclei (N) and transverse striations (S) in the sarcoplasm (H&E, ×400).

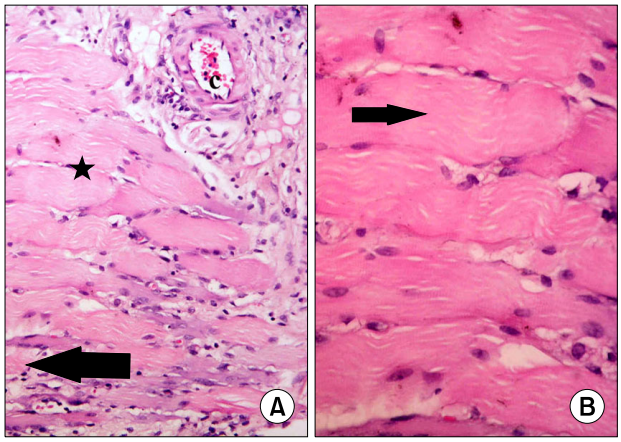

Fig. 3. (A) Skeletal muscle section of a rat in subgroup I2 showing atypical fibers (arrows) separated by few infiltrating cells (arrowhead). Some fibers exhibit dark nuclei (*) (H&E, ×200). (B) Higher magnification of the previous figure showing some fibers with partial loss of striations (arrows) (H&E, ×400).

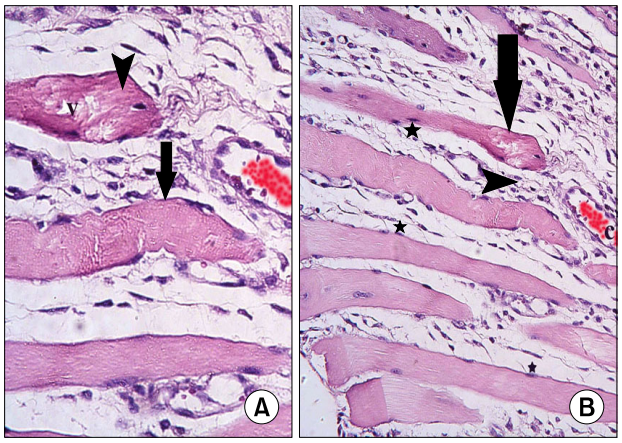

Fig. 2. (A) Skeletal muscle section of a rat in subgroup I1 showing atypical fibers (arrows) widely separated by infiltrating cells (arrowheads). Most fibers exhibit dark nuclei (*). Note a distended capillary (c) (H&E, ×200). (B) Higher magnification of the previous figure showing two fibers with partial loss of striations (arrows), one fiber exhibits strong acidophilic sarcoplasm (arrowheads) with focal vacuolations (v) (H&E, ×400).

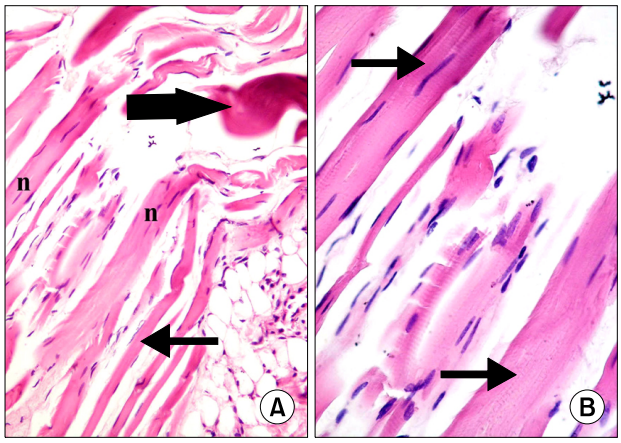

Fig. 4. (A) Skeletal muscle section of a rat in subgroup M1 showing some fibers exhibiting flat nuclei (thin arrows). Some of the nuclei (n) are centrally located. Note few atypical fibers (thick arrow) (H&E, ×200). (B) Higher magnification of the previous figure showing fibers with striations in some areas of the sarcoplasm (arrows) (H&E, ×400).

in some fibers on close observation (Fig. 3B).

In **subgroup M1** (Sacrifice 2weeks following injury and MCT), few atypical fibers were found. Other fibers exhibited multiple flat nuclei, some of these nuclei were centrally located (Fig. 4A). Striations appeared in some areas of the sarcoplasm on close observation (Fig. 4B). In subgroup M2 (Sacrifice 3 weeks following injury and MCT), few atypical fibers were seen surrounded by multiple typical fibers, some of which were observed with centrally located nuclei (Fig. 5A). Multiple fibers recruited striations in most areas of the sarcoplasm on close observation (Fig. 5B).

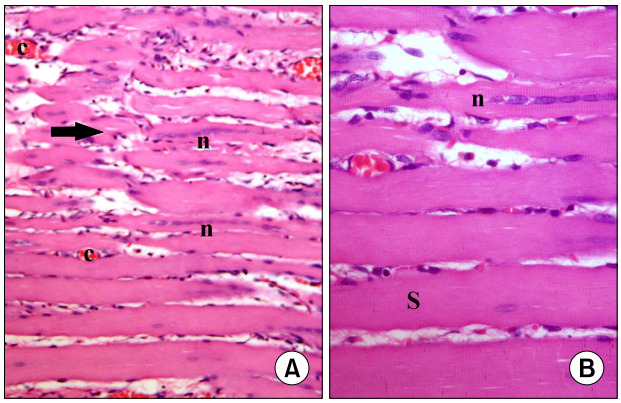

Fig. 5. (A) Skeletal muscle section of a rat in subgroup M2 showing few atypical (arrow) and multiple typical fibers, some of which with centrally located nuclei (n) (H&E, ×200). (B) Higher magnification of the previous figure showing multiple fibers with striations (S) in most areas of the sarcoplasm. Note some fibers with centrally located nuclei (n) (H&E, ×400).

Immunohistochemical results

Skeletal muscle sections of control rats demonstrated few alpha smooth muscle actin (α SMA) +ve spindle cells in between the muscle fibers (Fig. 6A). In subgroup I1 +ve spindle cells were found in the lining of blood vessels existing between atypical fibers (Fig. 6B). In subgroup I2 few +ve spindle cells were detected among some fibers with partial loss of striations (Fig. 6C). In subgroup M1 some +ve spindle cells were evident among some muscle fibers with centrally located nuclei (Fig. 6D). Subgroup M2 showed multiple +ve spindle cells among muscle fibers with striations in most areas of the sarcoplasm (Fig. 6E).

Skeletal muscle sections of control rats revealed few

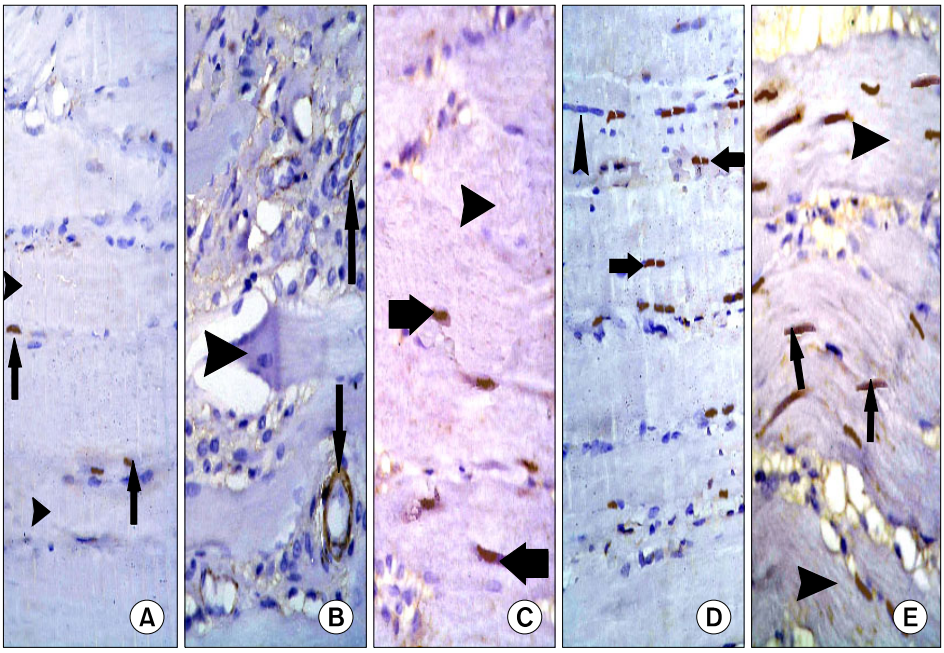

Fig. 6. (A) Skeletal muscle section of a control rat showing few alpha smooth muscle actin (α SMA) +ve spindle cells (arrows) in between skeletal muscle fibers (arrowheads) (α SMA immunostaining, ×400). (B) Skeletal muscle section of a rat in subgroup I1 showing α SMA +ve spindle cells (arrows) lining 2 blood vessels. Note atypical muscle fibers (arrowheads) (α SMA immunostaining, ×400). (C) Skeletal muscle section of a rat in subgroup I2 showing few α SMA +ve spindle cells (arrows) among some fibers with partial loss of striations (arrowheads) (α SMA immunostaining, ×400). (D) Skeletal muscle section of a rat in subgroup M1 showing some α SMA +ve spindle cells (arrows) among some muscle fibers with centrally located nuclei (arrowheads) (α SMA immunostaining, ×400). (E) Skeletal muscle section of a rat in subgroup M2 showing multiple α SMA +ve spindle cells (arrows) among muscle fibers with striations in most areas of sarcoplasm (arrowheads) (α SMA immunostaining, ×400).

CD34 +ve spindle cells at the periphery of the fibers (Fig. 7A). In subgroup I1, occasional +ve spindle and oval cells appeared around atypical fibers (Fig. 7B). In subgroup I2, some fields demonstrated few +ve spindle cells among muscle fibers (Fig. 7C). In subgroup M1 multiple +ve spindle cells were obvious at the periphery of muscle fibers (Fig. 7D). In subgroup M2 less numerous +ve spindle cells appeared at the periphery of the fibers (Fig. 7E).

Morphometric results

A significant ($p<0.05$) decrease in the mean area of atypical fibers was estimated in subgroup M1 compared to the injury subgroups I1 and I2. In addition, a significant ($p<0.05$) decrease was found in subgroup M2 compared to M1 (Table 1).

A significant ($p<0.05$) increase in the mean area% of alpha SMA+ve immunostaining was detected in subgroup M1 compared to the injury subgroups I1 and I2. In addition, a significant ($p<0.05$) increase was found in subgroup M2 compared to M1 (Table 1).

A significant ($p<0.05$) increase in the mean area% of CD34+ve immunostaining was estimated in subgroup M2

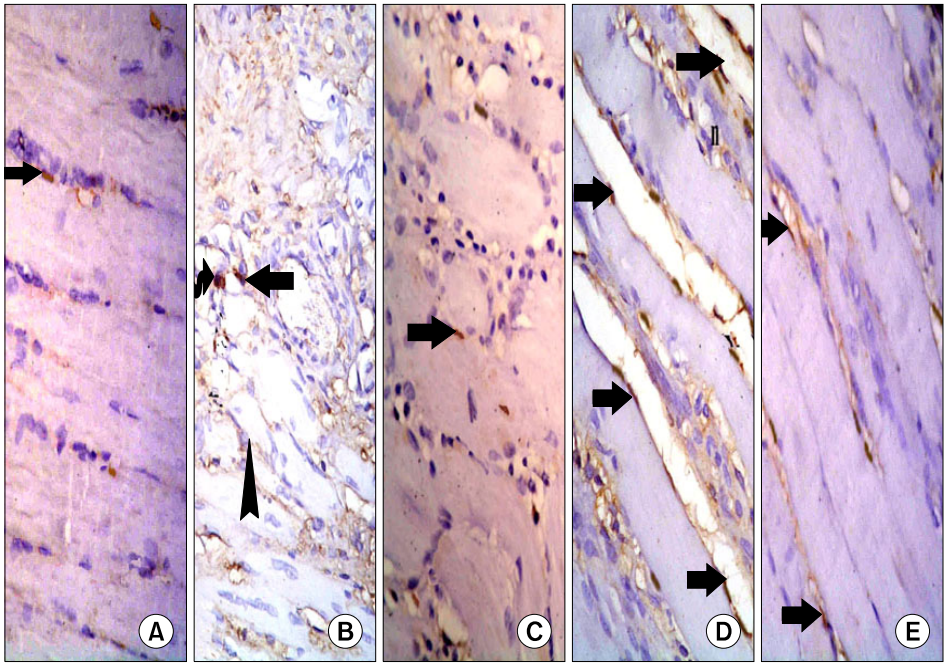

Fig. 7. (A) Skeletal muscle section of a control rat showing few CD34+ve spindle cells (arrows) at the periphery of the fibers (CD34 immunostaining, ×400). (B) Skeletal muscle section of a rat in subgroup I1 showing a +ve oval (curved arrow) and a +ve spindle (arrow) cells around atypical fibers (CD34 immunostaining, ×400). (C) Skeletal muscle section of a rat in subgroup I2 showing few +ve spindle cells (arrows) at the periphery of the fibers (CD34 immunostaining, ×400). (D) Skeletal muscle section of a rat in subgroup M1 showing multiple +ve spindle cells (arrows) at the periphery of the fibers. Note centrally located nuclei (n) (CD34 immunostaining, ×400). (E) Skeletal muscle section of a rat in subgroup M2 showing some +ve spindle cells (arrows) at the periphery of the fibers (CD34 immunostaining, ×400).

Table 1. Mean area of atypical fibers, mean area% of alpha SMA +ve cells and mean area% of CD34 +ve cells in control and experimental subgroups

Groups and Subgroups	Mean area of atypical fibers	Mean area% of alpha SMA +ve cells	Mean area% of CD34+ve cells
Control group	-	0.98±0.25	0.81±0.19
Subgroup I1	86.74±9.27	1.99±0.35	0.79±0.20
Subgroup I2	243.38±9.69	3.29±1.01	1.62±0.47
Subgroup M1	41.74±10.57*	5.67±0.43**	7.77±0.63$^{\$}$
Subgroup M2	13.62±3.39^	9.61±1.17$^{\#}$	3.95±0.26***

*significant compared to control group and subgroups I1, I2. ^significant compared to control group 1 and subgroups I1, I2, M1. **significant compared to control group and subgroups I1, I2. $^{\#}$significant compared to control group and subgroups I1, I2, M1. ***significant compared to control group and subgroups I1, I2. $^{\$}$significant compared to control group and subgroups I1, I2, M2.

compared to the injury subgroups I1 and I2. In addition, a significant ($p<0.05$) increase was found in subgroup M1 compared to M2 (Table 1).

Discussion

The current study demonstrated modulating effect of MCT on induced skeletal musle injury, which was associated with satellite cell existence in albino rat. This was evidenced by histological, immunohistochemical and morphometric studies.

In subgroup I1 (Sacrifice 2 weeks following muscle injury) the injured area demonstrated atypical fibers widely separated by infiltrating cells and distended capillaries. In accordance, it was stated that thermal injury of skeletal muscle of rat revealed greater interfiber distances and substantially increased amount of connective tissue (1). It was added that within the first week of traumatic muscle injury, granulated tissue and acute inflammation were found (9).

Most fibers contained dark nuclei, indicating apoptosis. The fibers revealed partial loss of striations and some fibers recruited strong acidophilic sarcoplasm with focal vacuolations on close observation. Crawford et al. (18) related injury of DNA to reactive oxygen species. In addition, similar degenerative cytoplasmic changes were described following muscle injury (2).

In subgroup I2 (Sacrifice 4 weeks following muscle injury), atypical fibers appeared separated by few infiltrating cells. Some fibers exhibited dark nuclei and partial loss of striations. The previous results indicated mild regression of degenerative changes. Concomitantly, it was documented that mononuclear cells can develop into a variety of different muscle cell lineages including myoblasts, satellite cells, and muscle derived stem cells (19).

In subgroup M1 (Sacrifice 2 weeks following injury and MCT), few atypical fibers were found. Other fibers exhibited multiple flat nuclei, some of these nuclei were centrally located. Striations appeared in some areas of the sarcoplasm. It was postulated that MCT limits muscle damage and inflammation, known as delayed onset muscle soreness in cases of injury (12). It was reported that neuro-muscular conductivity improved in response to MCT following muscle injury (20). It was recorded that Scs are the adult skeletal muscle stem cells that are quiescent, but during muscle regeneration proliferate and generate distinct daughter cells by segregating template DNA strands to the stem cell (21).

In subgroup M2 (Sacrifice 4 weeks following injury and MCT), few atypical fibers were seen surrounded by multiple typical fibers, some of which were observed with centrally located nuclei. Multiple fibers recruited striations in most areas of the sarcoplasm. These findings indicated progressive improvement of structural changes by MCT, proved by a significant decrease in mean area of atypical fibers. It was mentioned that Scs are located beneath the basal lamina of adult muscle fibers and are normally arrested in G0 of the cell cycle (22). They can be activated in response to stimuli, initiating a regenerative process, restoring the normal architecture of muscle within 2 weeks. This was confirmed by Francois et al. (23) who stated that survival of the satellite cells is a critical requirement for efficient muscle reconstitution following injury.

The regeneration capacity was assessed in the present work using α SMA. In subgroup I2 few +ve spindle cells were detected among some fibers with partial loss of striations. In subgroup M1 the +ve spindle cells were more evident and in subgroup M2 the +ve cells became multiple among the muscle fibers. This was confirmed by a significant increase in the mean area% of α SMA +ve cells. It was postulated that activation of muscle precursor cells is an important determinant for the efficiency of muscle regeneration. It was added that the main source of muscle precursor cells are satellite cells, which proliferate and migrate to the injured site (24).

In subgroup I1, occasional CD34+ve spindle and oval cells appeared around atypical fibers. Subgroup I2 demonstrated few +ve spindle cells among muscle fibers. On the other hand, in subgroup M1 multiple +ve spindle cells were obvious at the periphery of muscle fibers. While in subgroup M2 the +ve spindle cells appeared less. This was evidenced by a significant increase in the mean area% of CD34 +ve cells in microcurrent group. It was documented that Scs within the adult skeletal muscle are an enriched population of CD34+ve cells (16). It was proved that Scs are responsible for the regenerative potential of skeletal muscle (25). Alfaro et al. (26) considered that CD34 beyond being a stem cell marker, may play an important function in modulating stem cell activity. On the other hand, Ieronimakis et al. (6) noted a minority of satellite cells lacking CD34 to be described. Local SCs were documented as a promising treatment option for various diseases (27). In addition, histological examination suggested the therapeutic potential of local pluripotent cells in the treatment of ischemic diseases (28).

It can be commented that a definite therapeutic effect of the microcurrent was found on induced skeletal muscle injury. This effect was proved to be related to satellite cell activation.

Acknowledgments

The author acknowledges Dr Ahmed Hussein for his efforts in performing the microcurrent application.

Potential conflict of interest

The authors have no conflicting financial interest.

References

1. Oliveira Fd, Bevilacqua LR, Anaruma CA, Boldrini Sde C, Liberti EA. Morphological changes in distant muscle fibers following thermal injury in Wistar rats. Acta Cir Bras 2010;25:525-528
2. Gumerson JD, Michele DE. The dystrophin-glycoprotein complex in the prevention of muscle damage. J Biomed Biotechnol 2011;2011:210797
3. Kim MY, Kwon DR, Lee HI. Therapeutic effect of microcurrent therapy in infants with congenital muscular torticollis. PM R 2009;1:736-739
4. Lee BY, Al-Waili N, Stubbs D, Wendell K, Butler G, Al-Waili T, Al-Waili A. Ultra-low microcurrent in the management of diabetes mellitus, hypertension and chronic wounds: report of twelve cases and discussion of mechanism of action. Int J Med Sci 2009;7:29-35
5. Aliyev RM, Geiger G. Cell-stimulation therapy of lateral epicondylitis with frequency-modulated low-intensity electric current. Bull Exp Biol Med 2012;152:653-655
6. Ieronimakis N, Balasundaram G, Rainey S, Srirangam K, Yablonka-Reuveni Z, Reyes M. Absence of CD34 on murine skeletal muscle satellite cells marks a reversible state of activation during acute injury. PLoS One 2010;5:e10920-e10935.
7. Armand AS, Laziz I, Djeghloul D, Lécolle S, Bertrand AT, Biondi O, De Windt LJ, Chanoine C. Apoptosis-inducing factor regulates skeletal muscle progenitor cell number and muscle phenotype. PLoS One 2011;6:e27283-e27307
8. Riuzzi F, Sorci G, Beccafico S, Donato R. S100B engages RAGE or bFGF/FGFR1 in myoblasts depending on its own concentration and myoblast density. Implications for muscle regeneration. PLoS One 2012;7:e28700-e28717
9. Lee YS, Kwon ST, Kim JO, Choi ES. Serial MR imaging of intramuscular hematoma: experimental study in a rat model with the pathologic correlation. Korean J Radiol 2011;12:66-77
10. Passarini Junior JR, Gaspi FO, Neves LM, Esquisatto MA, Santos GM, Mendonça FA. Application of Jatropha curcas L. seed oil (Euphorbiaceae) and microcurrent on the healing of experimental wounds in Wistar rats. Acta Cir Bras 2012;27:441-447
11. Mehmandoust FG, Torkaman G, Firoozabadi M, Talebi G. Anodal and cathodal pulsed electrical stimulation on skin wound healing in guinea pigs. J Rehabil Res Dev 2007; 44:611-618
12. Curtis D, Fallows S, Morris M, McMakin C. The efficacy of frequency specific microcurrent therapy on delayed onset muscle soreness. J Bodyw Mov Ther 2010;14:272-279
13. Kiernan JA. Histological and histochemical methods: theory and Practice. 3rd ed. London: Hodder Arnold Publishers; 2001. 111-162
14. Elia A, Charalambous F, Georgiades P. New phenotypic aspects of the decidual spiral artery wall during early post-implantation mouse pregnancy. Biochem Biophys Res Commun 2011;416:211-216
15. Zhou JH, Cao LH, Liu JB, Zheng W, Liu M, Luo RZ, Han F, Li AH. Quantitative assessment of tumor blood flow in mice after treatment with different doses of an antiangiogenic agent with contrast-enhanced destruction-replenishment US. Radiology 2011;259:406-413
16. Pasut A, Oleynik P, Rudnicki MA. Isolation of muscle stem cells by fluorescence activated cell sorting cytometry. Methods Mol Biol 2012;798:53-64
17. Emsley R, Dunn G, White IR. Mediation and moderation of treatment effects in randomised controlled trials of complex interventions. Stat Methods Med Res 2010;19:237-270
18. Crawford RS, Albadawi H, Atkins MD, Jones JJ, Conrad MF, Austen WG Jr, Fink MP, Watkins MT. Postischemic treatment with ethyl pyruvate prevents adenosine triphosphate depletion, ameliorates inflammation, and decreases thrombosis in a murine model of hind-limb ischemia and reperfusion. J Trauma 2011;70:103-110
19. Mu X, Peng H, Pan H, Huard J, Li Y. Study of muscle cell dedifferentiation after skeletal muscle injury of mice with a Cre-Lox system. PLoS One 2011;6:e16699-e16707
20. Lazarenko NN, Gerasimenko MIu. The application of multichannel electrostimulation and nivalin electrophoresis for the rehabilitative treatment of the patient following plastic surgery in the facial region. Vopr Kurortol Fizioter Lech Fiz Kult 2011;(5):39-44
21. Rocheteau P, Gayraud-Morel B, Siegl-Cachedenier I, Blasco MA, Tajbakhsh S. A subpopulation of adult skeletal muscle stem cells retains all template DNA strands after cell division. Cell 2012;148:112-125
22. Robson LG, Di Foggia V, Radunovic A, Bird K, Zhang X, Marino S. Bmi1 is expressed in postnatal myogenic satellite cells, controls their maintenance and plays an essential role in repeated muscle regeneration. PLoS One 2011;6:e27116-e27126
23. François S, D'Orlando C, Fatone T, Touvier T, Pessina P, Meneveri R, Brunelli S. Necdin enhances myoblasts survival by facilitating the degradation of the mediator of apoptosis CCAR1/CARP1. PLoS One 2012;7:e43335-e43345
24. Mu X, Urso ML, Murray K, Fu F, Li Y. Relaxin regulates MMP expression and promotes satellite cell mobilization during muscle healing in both young and aged mice. Am J Pathol 2010;177:2399-2410
25. Di Foggia V, Robson L. Isolation of satellite cells from single muscle fibers from young, aged, or dystrophic muscles. Methods Mol Biol 2012;916:3-14
26. Alfaro LA, Dick SA, Siegel AL, Anonuevo AS, McNagny KM, Megeney LA, Cornelison DD, Rossi FM. CD34 promotes satellite cell motility and entry into proliferation to

facilitate efficient skeletal muscle regeneration. Stem Cells 2011;29:2030-2041
27. Zhao X, Huang L. Cardiac stem cells: A promising treatment option for heart failure. Exp Ther Med 2013;5:379-383
28. Rajabi-Zeleti S, Jalili-Firoozinezhad S, Azarnia M, Khayyatan F, Vahdat S, Nikeghbalian S, Khademhosseini A, Baharvand H, Aghdami N. The behavior of cardiac progenitor cells on macroporous pericardium-derived scaffolds. Biomaterials 2014;35:970-982